Harmonic Generation by Femtosecond Laser-Solid Interaction: A Coherent "Water-Window" Light Source?

Paul Gibbon
Max-Planck-Gesellschaft, Research Unit "X-Ray Optics," Friedrich Schiller University Jena, Max-Wien-Platz 1, D-07743 Jena, Germany
(Received 20 March 1995; revised manuscript received 17 November 1995)

The generation of harmonics by short, intense laser pulses reflected from a solid-density plasma is investigated using particle-in-cell simulation. High irradiance, obliquely incident *p*-polarized light generates harmonics via relativistic electrons dragged across the vacuum-solid interface. This mechanism does not exhibit the limitation previously predicted for lower intensities of a maximum harmonic "cutoff" $n_{\max} = \omega_p/\omega_0$. For $I\lambda^2 > 10^{19}\ \mathrm{W\,cm^{-2}}\ \mu\mathrm{m}^2$ and modest shelf densities $N_e/N_{\mathrm{crit}} = 10$, at least 60 harmonics can be generated with power efficiencies $P_n/P_1 > 10^{-6}$, suggesting coherent MW x rays with $\lambda \sim 4$ nm could be generated with a KrF (248 nm) pump.

PACS numbers: 52.40.Nk, 52.50.Jm, 52.65.Rr

The search for a coherent, tunable source of x rays has been underway for some years in a variety of different fields [1]. Such light sources, by virtue of their short wavelength and high resolving power, have numerous potential applications in the field of x-ray imaging. New possibilities for short-wavelength generation have recently emerged through advances in short-pulse, multiterawatt laser technology [2]. Laser pulses focused on solids or in gases with intensities exceeding $10^{18}\ \mathrm{W\,cm^{-2}}$ rapidly ionize the targeted medium: The well-known "figure-8" motion of the electrons in the plasma thus created may be strongly relativistic, a feature that can in principle be exploited for generating short-wavelength radiation [3]. In underdense plasmas, where the electron density N_e is below the critical density N_c for an electromagnetic (EM) wave with frequency ω_0 (where $\omega_0^2 = 4\pi e^2 N_c/m_e$), the efficiency of this process is reduced by the collective fluid response to the particle orbits, and by dephasing of the harmonics relative to the pump [4]. In the opposite case where the plasma is overdense with $N_e > N_c$, harmonics can be generated in the reflected light by the nonlinear mixing of transverse and longitudinal oscillations near the critical surface.

This mechanism was demonstrated in the early 1980s in a series of experiments by Carman *et al.* [5,6] with a high-irradiance CO_2 laser, in which over 40 harmonics were detected. Subsequent theoretical work based on Lagrangian fluid analysis in a steplike density profile [7] predicted a cutoff in the harmonic spectrum given by $n_{\max} = \sqrt{N_u/N_c}$, N_u being the upper shelf density of the plasma. This result appeared to be consistent with 2D particle-in-cell (PIC) simulations made by Carman, Forslund, and Kindel [5], thus implying that the maximum harmonic number could be used as an indirect means of determining the plasma density. Furthermore, assuming that the density profile is in pressure balance with the laser, then $n_{\max} \propto (I\lambda^2/T_e)^{1/2}$, where I, λ, and T_e are the laser intensity, laser wavelength, and plasma temperature, respectively. While this scaling might be appropriate for nanosecond interactions, in which there is ample time for the ions to respond, it is questionable on the subpicosecond time scale. Instead, we expect a shock to form due to the superior laser pressure, so the maximum density will be a little more than that determined by the highest ionization state. In this case, $n_{\max} = \omega_p/\omega_0$, and the minimum attainable wavelength would be $\lambda_{\min} \sim 1/n_{\max}\omega_0 \sim 1/\sqrt{N_e}$, i.e., *independent* of the initial wavelength and intensity. There were, however, two factors which severely restricted the PIC simulations reported in Ref. [5]: First, the temporal and spatial step sizes used were too large to resolve more than 10 harmonics; second, the noise in the computed Fourier spectra was at the same level as the harmonic intensities near the plasma frequency ω_p, making it difficult to distinguish a genuine rolloff in the spectrum from a gradual merging with the white background signal.

During the past year, a fresh round of experiments has begun which will extend the study of harmonic generation to the high-intensity, femtosecond regime [8,9]. In anticipation of these experiments, new results are reported here on a series of simulations in which the limitations of 2D codes are overcome using a recently developed boosted-frame-of-reference 1D PIC code [10]. This method reduces the 2D (x, y), periodic system to one spatial dimension by transforming to a simulation frame in which the EM wave vector perpendicular to the density gradient vanishes: $k_y' = 0$. In this way, the same problem can be studied with over 30 times the temporal and spatial resolution—theoretically sufficient to "detect" several hundred harmonics. In contrast to the earlier work, we find no cutoff at ω_p: the number of distinguishable harmonics simply depends on the irradiance and the signal-to-noise ratio of the simulation. Indeed, for modest plasma densities, $N_e/N_c = 10$, it is found that over 50 harmonics can be generated (as opposed to 3, implied by the cutoff argument) for irradiances between 10^{18} and

 0031-9007/96/76(1)/50(4)$06.00 © 1995 The American Physical Society

10^{19} W cm^{-2} μm^2, with efficiencies $\eta_n \equiv I_n/I_0 > 10^{-6}$. The mechanism is more efficient than the closely related $\boldsymbol{v} \wedge \boldsymbol{B}$ mechanism recently proposed by Wilks, Kruer, and Mori [11]. Lower-order harmonics ($n \leq 6$) from p-polarized light were observed in analogous oblique-incidence PIC simulations by Bulanov, Naumova, and Pegoraro [12].

In most of the simulations that follow, the laser was p polarized and 45° incident on a step profile with density $N_e/N_c = 10$ and temperature $T_e = 625$ eV. The ions were mobile with $m_i/Zm_e = 7000$ and $T_i/T_e = 1/10$. Around 6000 mesh points were used, and 64k electrons and ions. The total system size was between $30c/\omega_0$ and $60c/\omega_0$, i.e., large enough to prevent particles reaching the left-hand (vacuum) boundary; the plasma was initialized in a region $\sim 10c/\omega_0$ long at the right-hand boundary. The time step used was typically less than $10^{-2}\omega_0^{-1}$ and $\Delta x = c\Delta t$, which was sufficient to resolve modes $\omega_{\max} = ck_{\max} \simeq 300\omega_0$. The laser was ramped up over several laser periods and then held constant; this permits the scaling of diagnostic variables such as the harmonic efficiency to be obtained in a straightforward manner.

Time-integrated spectra of the reflected EM wave are shown in Fig. 1 for two different irradiances at *fixed* upper shelf density and temperature. No attempt was made to match the laser and plasma pressures. Notice how the harmonics for $I\lambda^2 = 2 \times 10^{17}$ W cm^{-2} μm^2 fall off rapidly into the background noise: only 4 or 5 harmonics are clearly visible. The feature between $4\omega_0$ and $5\omega_0$ is due to emission from the upper plasma shelf, and can be supressed by taking a larger N_e/N_c (which was 10 in this case). The spectrum for $I\lambda^2 = 2 \times 10^{18}$ W cm^{-2} μm^2 clearly rules out any suggestion of a cutoff at ω_p which might be inferred from the first result.

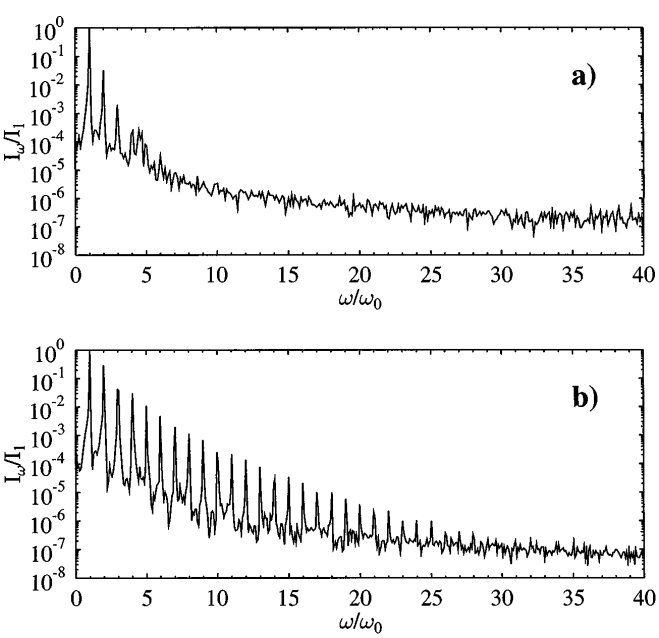

FIG. l. Spectrum of reflected electromagnetic wave for (a) $I\lambda^2 = 2 \times 10^{17}$ W cm^{-2} μm^2 and (b) $I\lambda^2 = 2 \times 10^{18}$ W cm^{-2} μm^2.

To trace the physical mechanism behind the harmonic generation, a second set of simulations was made with *fixed* ions in an exponential profile with scale length $L/\lambda = 0.01$. Under these conditions, the absorption is constant and fairly low [(10–15)%] [10], and comprises particles that have undergone "vacuum excursions," i.e., electrons that have been pulled out and accelerated back into the plasma, where they free stream through to the right-hand boundary of the simulation region [13]. It is reasonable to suppose that these particles are also responsible for harmonic generation, even if they only do one return trip into vacuum; a picture that shares much in common with the periodic, nonlinear fluid motion envisaged in Ref. [7]. To demonstrate this, the labels of energetic electrons falling within a narrow energy band close to $U \sim p_{\text{osc}}^2/m_e$ were stored at the end of a simulation. The quiver momentum p_{osc} is given by $p_{\text{osc}}/m_e c \simeq (I\lambda^2/1.38 \times 10^{18}\ \text{W cm}^{-2}\ \mu\text{m}^2)^{1/2}$. The simulation was then repeated, and the same list was used to monitor the position x, momenta p_x, and acceleration $a_x = d^2x/dt^2$ of the "interesting" particles.

An example of one such group of like trajectories is shown in Fig. 2(a). The corresponding impulselike accelerations in Fig. 2(b) are characteristic of harmonic generation. These orbits are consistent with the experimental observations in Ref. [6], and are in qualitative agreement

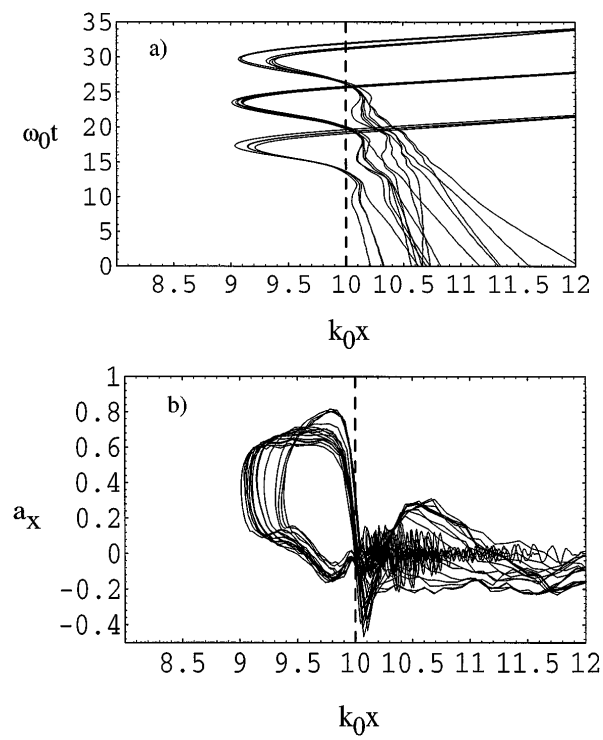

FIG. 2. (a) Trajectories and (b) accelerations $a_x = d^2x/dt^2$ of particles undergoing vacuum excursions for a fixed-ion simulation with $I\lambda^2 = 5 \times 10^{17}$ W cm^{-2} μm^2, $N_e/N_c = 10$, and $L/\lambda = 0.01$. The solid density is at $k_0 x = 10$.

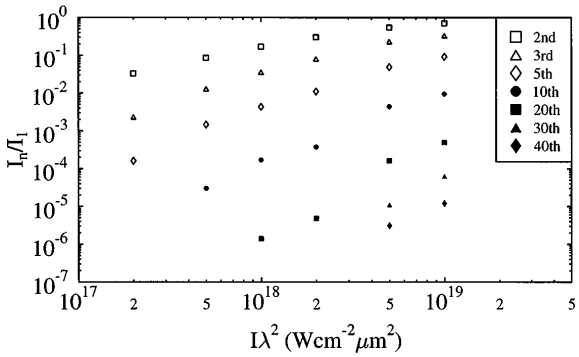

FIG. 3. Efficiency of selected harmonics as a function of irradiance.

with the model of Bezzerides *et. al.* [7]. However, it is also evident that the particles receiving this reverse kick as they re-enter the plasma are not turned around, but continue into the solid where they are ultimately absorbed. This process is therefore kinetic: The reversal in the acceleration suggests a bunching of the electrons as they re-enter, i.e., a sharp, periodic density spike. Fourier analysis of the harmonic current sources shows that their maxima are located just inside the overdense plasma boundary [at $x = 10$ in Fig. 2(a)].

Returning to the main set of mobile-ion simulations, selected harmonic powers relative to the reflected fundamental mode P_1 are given in Fig. 3. The 2nd to 5th harmonics start to become saturated between 10^{18} and 10^{19} W cm^{-2} μm^2 due to the fact that the transverse velocity v_y approaches c, an effect also seen for odd harmonics generated at normal incidence by the relativistic $\boldsymbol{v} \wedge \boldsymbol{B}$ mechanism [11].

It should be noted that the $\boldsymbol{v} \wedge \boldsymbol{B}$ mechanism can generate odd *and* even harmonics at oblique incidence. For *p*-polarized light, the current sources for the 2nd and 3rd harmonics are $\boldsymbol{J}^p_{2\omega} = \boldsymbol{v}^{\parallel}_{\omega} n_\omega + \boldsymbol{v}^{\perp}_{2\omega} n_0$, $\boldsymbol{J}^p_{3\omega} = \boldsymbol{v}^{\perp}_{2\omega} n_\omega + \boldsymbol{v}^{\parallel}_{\omega} n_{2\omega}$, where $\boldsymbol{v}^{\parallel}$ and $\boldsymbol{v}^{\perp}$ denote the velocity components normal and perpendicular to the laser electric field, respectively, and we have expanded the density in a Fourier series: $N_e = n_0 + n_\omega + n_{2\omega}$. For *s*-polarized light, the density-bunching term n_ω vanishes, and we have $\boldsymbol{J}^s_{2\omega} = \boldsymbol{v}^{\perp}_{2\omega} n_0$, $\boldsymbol{J}^s_{3\omega} = \boldsymbol{v}^{\parallel}_{\omega} n_{2\omega}$, which generate *s*- (TE) and *p*-polarized (TM) even and odd harmonics, respectively. We can thus distinguish the vacuum-excursion and $\boldsymbol{v} \wedge \boldsymbol{B}$ mechanisms by comparing harmonics from *p*- and *s*-polarized light, as shown in Fig. 4. At small angles, the $\boldsymbol{v} \wedge \boldsymbol{B}$ current sources dominate, and the efficiencies of the odd harmonics for *s* and *p* light are comparable. At large angles, however, the efficiences are 1–2 orders of magnitude higher for *p* due to the contribution from vacuum excursions (Fig. 2).

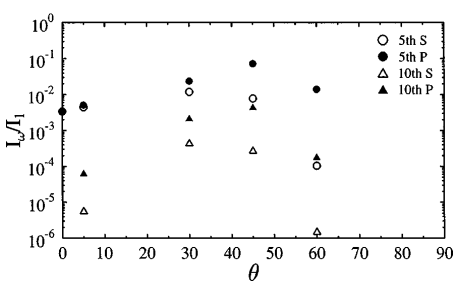

FIG. 4. Efficiency of 5th and 10th harmonics as a function of incidence angle for *p*- and *s*-polarized light at 10^{19} W cm^{-2} μm^2. The other parameters were $n_e/n_c = 5$, $L/\lambda = 0.02$, $m_i/m_e = \infty$, and $T_e = 1$ keV.

The relative power spectra for four different irradiances are summarized in Fig. 5. For large $n = \omega_n/\omega_0$, the spectrum rolloff appears to vary as $O(n^{-5})$. Combining this with the $I\lambda^2$–scaling from Fig. 3 of $O(I\lambda^2)^{2-2.5}$ in the same limit, we arrive at a rough expression for the efficiency of high-order harmonics:

$$\eta_n \simeq 9 \times 10^{-5} \left(\frac{I\lambda^2}{10^{18}\ \mathrm{W\,cm^{-2}}\ \mu\mathrm{m}^2} \right)^2 \left(\frac{n}{10} \right)^{-5}.$$

For $I\lambda^2 \geq 10^{19}$ W cm^{-2} μm^2 and large incidence angles, the efficiency can be very high (Fig. 6). For example, the 30th harmonic has $\eta \simeq 3 \times 10^{-5}$, which would yield 0.5 GW at 33 nm for a 1 μm, 15 TW pump focused to a spot size of 10 μm. Transmitted spectra are also observed containing harmonics $n > \sqrt{N_e/N_c}$ with intensities between 1/100 (high end) and 1/10 (low end) of the reflected counterparts.

A further significant feature is that over 60 harmonics are clearly observed for *p*-polarized light at this irradiance, which implies that coherent radiation within the so-called "water window" could be generated with a sufficiently intense (i.e., 1.6×10^{20} W cm^{-2}) KrF pump. In this case, the 60th harmonic would have a wavelength of 4.1 nm, well within the "water-window" range (2.3–4.4 nm). Harmonics are distinguishable down to about 3.5 nm, below which they get drowned in the simulation noise. This does not mean that they would be undetectable experimentally; rather, it reflects the limits of the present simulations.

Physically, the harmonic efficiency may be impaired by any process which upsets the coherence of the electron orbits across the vacuum-plasma interface. This favors

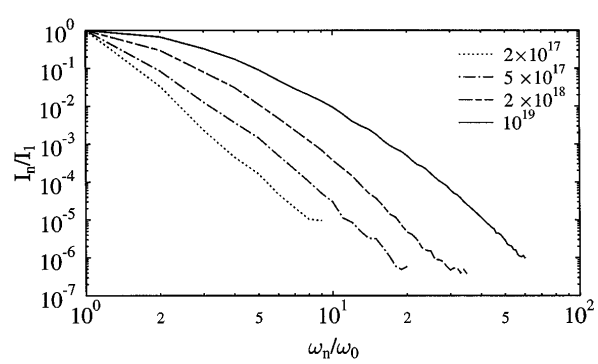

FIG. 5. Power spectra for mobile-ion simulations at various irradiances.

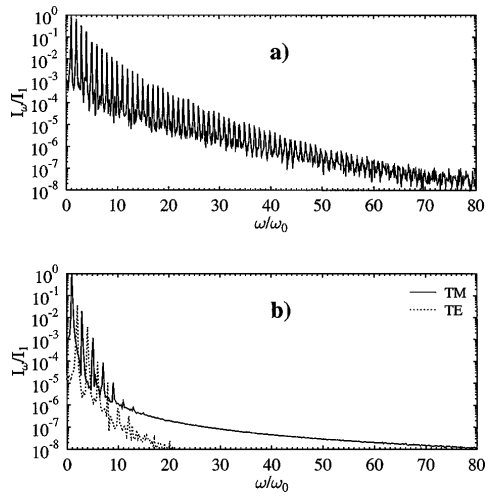

FIG. 6. Harmonic spectra at $I\lambda^2 = 10^{19}$ W cm^{-2} μm^2 for (a) *p*-polarized light and (b) *s*-polarized light.

the following: (i) short pulse lengths to avoid formation of an underdense shelf and subsequent high absorption [14] and (ii) broad spot sizes, to avoid denting the surface and lateral deviations of the electrons from their "1D" paths [15]. On the other hand, Rayleigh-Taylor-like surface rippling would scatter harmonics over a broad angular range relative to the specular direction, and would blur the distinction between *s*- and *p*-polarized light implied by Fig. 6 . Finite density gradients formed by a prepulse (or the leading edge of the main pulse) might also prevent efficient harmonic generation if the pulse duration is too short for profile steepening to take place.

In summary, we have revisited the problem of harmonic generation by reflection of intense light from overdense plasmas. Using a short cut to reduce a 2D problem to 1D while retaining the essential physics, we have been able to perform simulations with the necessary spatial and temporal resolution required to model the generation of high-order harmonics in laser-plasma interaction. For *p*-polarized light at large incidence angles harmonics originate from electrons which traverse the vacuum-solid interface, creating periodic density bunching as they return, before getting absorbed further into the solid. In contrast to previous works which considered lower laser intensities, no harmonic cutoff is found for the reflected light at the plasma frequency corresponding to the upper density shelf. Indeed, it is demonstrated for the first time that coherent, water-window x rays could be efficiently produced using femtosecond laser technology which will be available in the near future. Existing high-contrast multiterawatt laser systems should be capable of producing short-pulse, tunable UV radiation at MW–GW power levels.

The author acknowledges enlightening discussions on the subject of harmonic generation with J. M. Rax, T. Auguste, and P. Monot. This work was performed in part at C.E.A.-Centre d'Etudes de Saclay, France, supported by the European Human Capital and Mobility Programme.

[1] D. L. Matthews and M. D. Rosen, Sci. Am. **12**, 86 (1988); E. Fill, Appl. Phys. B **58**, 1 (1994), and references therein; A. L'Huillier and P. Balcou, Phys. Rev. Lett. **70**, 774 (1993).
[2] M. D. Perry and G. Mourou, Science **264**, 917 (1994); M. M. Murnane, H. C. Kapteyn, M. D. Rosen, and R. W. Falcone, Science **251**, 531 (1991).
[3] E. S. Sarachik and G. T. Schappert, Phys. Rev. D **1**, 2738 (1970); E. Esarey, P. Sprangle, and S. K. Ride, Phys. Rev. E **48**, 3003 (1993).
[4] J. M. Rax and N. J. Fisch, Phys. Rev. Lett. **69**, 772 (1992); W. B. Mori, C. D. Decker, and W. P. Leemans, IEEE Trans. Plasma Sci. **21**, 1 (1993); E. Esarey *et al.*, *ibid.* **21**, 95 (1993).
[5] R. L. Carman, D. W. Forslund, and J. M. Kindel, Phys. Rev. Lett. **46**, 29 1981).
[6] R. L. Carman, C. K. Rhodes, and R. F. Benjamin, Phys. Rev. A **24**, 2649 (1981).
[7] B. Bezzerides, R. D. Jones, and D. W. Forslund, Phys. Rev. Lett. **49**, 202 (1982);C. Grebogi, V. K. Tripathi, and H.-H. Chen, Phys. Fluids **26**, 1904 (1983).
[8] S. Kohlweyer *et al.*, Opt. Commun. **117**, 431 (1995); D. von der Linde *et al.*, Phys. Rev. A **52**, R25 (1995).
[9] P. Norreys *et al.* (to be published).
[10] P. Gibbon and A. R. Bell, Phys. Rev. Lett. **68**, 1535 (1992).
[11] S. C. Wilks, W. L. Kruer, and W. B. Mori, IEEE Trans. Plasma Sci. **21**, 120 (1993).
[12] S. V. Bulanov, N. M. Naumova, and F. Pegoraro, Phys. Plasmas **1**, 745 (1994).
[13] F. Brunel, Phys. Rev. Lett. **59**, 52 (1987).
[14] P. Gibbon, Phys. Rev. Lett. **73**, 664 (1994).
[15] S. C. Wilks, W. L. Kruer, M. Tabak, and A. B. Langdon, Phys. Rev. Lett. **69**, 1383 (1992).